First publ. in: Zeitschrift für Physik B - Condensed Matter 85 (1991), S. 79-86

Specific heat of $Eu_xSr_{1-x}Te$

E. Scheer, J. Wosnitza, and H. v. Löhneysen

Physikalisches Institut, Universität Karlsruhe, Engesserstrasse 7, W-7500 Karlsruhe, Federal Republic of Germany

Received May 3, 1991

In this paper, we report on measurements of the specific heat C of single-crystalline $Eu_xSr_{1-x}Te$ at temperatures between 60 mK and 15 K and in magnetic fields up to 6 T. Pure antiferromagnetic EuTe shows unusual critical behavior in the vicinity of the Néel temperature $T_N = 9.8$ K with a positive critical exponent instead of the 3d-Heisenberg exponent $\alpha = -0.12$. Possible reasons for this discrepancy between theory and experiment include magnetic anisotropy effects due to magnetic dipole-dipole interactions, which may give rise to a cross-over of the critical behavior very close to T_N. This anisotropy is also seen in the specific heat below 1 K where an exponential decay of C is observed, and in the dependence of the magnetic susceptibility on the direction of the applied field. With increasing dilution of EuTe with nonmagnetic Sr, the critical behavior changes: α becomes negative and decreases continuously towards $\alpha \approx -1$ at $x \approx x_c$. This concentration dependence of α was previously observed in the diluted ferromagnetic system $Eu_xSr_{1-x}S$. Our data thus support that the apparent change in the critical behavior depends on the degree of disorder. Samples with concentration x lower than the critical concentration x_c reveal spin-glass behavior in the specific heat. In addition, the dependence of T_N on magnetic fields is discussed. The data yield a normalized magnetic phase boundary $B_c(T)/B_c(T=0)$ vs. $T_N(B)/T_N(B=0)$ which is independent of concentration.

I. Introduction

The Eu monochalcogenides EuX (X = O, S, Se, Te) are known as magnetic model substances with localized magnetic moments. The Eu^{++}-ion in EuX has only a spin moment $S = 7/2$ and, following Hund's rules, has an $^8S_{7/2}$ groundstate. All these systems crystallize in the NaCl structure. Their magnetic properties are determined by exchange interactions between nearest neighbors (J_1) and next-nearest neighbors (J_2) [1].

EuO and EuS are ferromagnets at low temperatures and correspond very well to the predictions for 3d-Heisenberg magnets in many static properties [1–5] while for dynamic properties dipolar interactions have to be taken into account [6]. EuSe shows complicated metamagnetic behavior [7]. EuTe orders antiferromagnetically with a Néel temperature $T_N = 9.8$ K because the antiferromagnetic J_2 exceeds J_1 ($J_1/k_B = 0.06$ K, $J_2/k_B = -0.16$ K) [1, 8]. The magnetic structure is of the second kind (MnO structure) with the (111) planes as easy planes. The ratio between anisotropy field due to magnetic dipole-dipole interaction and interaction field is $H_A/H_E \approx 0.1$. In small magnetic fields $B_f \approx 0.08$ T (parallel [100]) EuTe flops into the canted phase with the spins still in the easy planes but directed nearly perpendicular to each other and to the applied magnetic field. Increasing field aligns the spins more and more and at the critical field $B_c = 7.4$ T at $T = 0$ a second order phase transition to the paramagnetic state occurs. As a result of an additional in-plane anisotropy, the [11$\bar{2}$]-directions are the easy directions [9, 10]. The magnetic phase diagram of EuTe has been investigated theoretically by mean-field and Monte Carlo calculations [11].

The EuX systems are very suitable for the investigation of the properties of diluted magnets by replacing statistically the Eu atoms by nonmagnetic Sr [2, 4, 12]. Due to the similar lattice constants (EuTe: $a = 6.598$ Å [8]; SrTe: $a = 6.659$ Å [13]) homogeneous single crystals of each concentration x can be produced. Because of the competing interactions J_1 and J_2 in $Eu_xSr_{1-x}S$ and $Eu_xSr_{1-x}Te$, spin-glass order occurs below the critical concentration x_c. The magnetic phase diagram (Fig. 1) of $Eu_xSr_{1-x}Te$ has been determined by measurements of the dc-magnetization for samples with $x \geqq 0.85$ and of the ac-susceptibility for $x \leqq 0.6$ [12]. The critical concentration is not well established, $0.45 \leqq x_c \leqq 0.5$.

In this paper, we report on high-resolution measurements of the specific heat of $Eu_xSr_{1-x}Te$ in the concentration range $0.3 \leqq x \leqq 1$. The samples are of the same source as used in [12]. The magnetic transition manifests itself in a sharp anomaly of the specific heat. These anomalies are used to confirm the phase diagram Fig. 1.

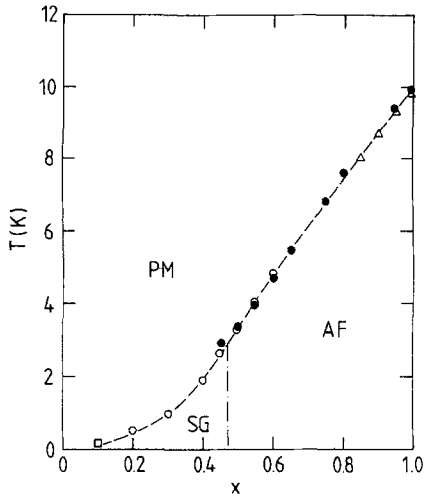

Fig. 1. Magnetic phase-diagram of $Eu_xSr_{1-x}Te$, open symbols from [12] (triangles: Faraday magnetometer, circles: dc magnetization, square: ac magnetization), closed symbols: this work (specific heat)

The magnetic specific heat in the vicinity of the critical temperature $T_c = T_N$ can be described by the function $C_M \propto |(T - T_c)/T_c|^{-\alpha}$. Renormalization-group (RG) theory requires α to be universal, i.e., α depends only on a few basic properties of the system (dimension d, number of components of the order parameter, range of the interaction). For 3d-Heisenberg magnets with short-range interaction, $\alpha = -0.12$ [14] is obtained as confirmed experimentally for EuS [3] and antiferromagnetic $RbMnF_3$ [15].

The influence of disorder on the critical behavior was first discussed by Harris [16]. The Harris criterion states that if $\alpha_0 < 0$ in the pure system, small disorder does not change the critical behavior, whereas for systems with $\alpha_0 > 0$, disorder causes a change to a new fixed point with different critical exponents. In a previous investigation of $Eu_xSr_{1-x}S$, deviations from $\alpha_0 = -0.12$ were observed even for small Sr concentration ($x = 0.95$), with a continuous decrease of α towards $\alpha \approx -1$ near the critical concentration [4]. This apparent contradiction to the Harris criterion might have two reasons: (1) "strong" disorder is present already for $x = 0.95$ because of the simultaneous presence of ferromagnetic and antiferromagnetic couplings, and/or (2) the determined exponents are effective exponents for the experimentally attainable reduced temperatures $|t| > 0.001$, and a cross-over to the pure exponent occurs closer to the transition temperature [17, 18]. In any case, it appeared worthwhile to look for possible changes of α upon dilution in a different, antiferromagnetic system.

Another point of interest is concerned with low-energy excitations as measured with the specific heat at very low temperatures well below T_N. These measurements will be compared to other Eu-dilution systems as $Eu_xSr_{1-x}S$ [19] and the anisotropic antiferromagnetic series $Eu_xSr_{1-x}As_3$ [20, 21].

Finally, the magnetic-field dependence of T_N of the whole series will be compared to recent mean-field and Monte Carlo calculations for EuTe [11].

The paper is organized as follows: Section II gives experimental details; in Sect. III.A the results of the low-temperature measurements without external magnetic field are presented and discussed; Sect. III.B describes the critical behavior; and Sect. III.C gives a short survey of the specific-heat measurements in magnetic fields.

II. Experimental details

The single crystals are obtained from K. Fischer at the Institut für Festkörperforschung, Forschungszentrum Jülich. They were grown in Ar atmosphere at ≈ 2200 °C in closed tungsten crucibles. The samples have roughly orthorhombic shape with mass between 30 mg and 130 mg. The specific-heat measurements are performed in a ^4He and a dilution refrigerator by a standard heat-pulse technique, described elsewhere [19]. Calibrated carbon resistors are used as thermometers. The steep $R(T)$ characteristic of the thermometers allows to apply heat pulses much smaller than 1 mK in the vicinity of T_N. The absolute accuracy of the specific heat is about 1% at low temperatures and 3% at high temperatures ($T > 12$ K). The temperature resolution is better than 0.01 mK at the antiferromagnetic transition.

The magnetic susceptibility is measured with a SQUID-dc-magnetometer between 4.2 K and room temperature in magnetic fields around 10 mT. At higher temperatures $T > 60$ K EuTe shows a Curie-Weiss susceptibility with an effective paramagnetic moment $p_{\text{eff}} = 7.84$ in good agreement with the theoretical value $p_{\text{eff}} = 7.94$ for Eu^{++} with $J = S = 7/2$.

III. Results and discussion

III.A. Specific heat at low temperatures without external magnetic field

Figure 2 displays the specific heat C at low temperatures $T < 3$ K of the samples with $x = 1$, $x = 0.65$, and $x = 0.3$ on a log C vs. log T plot. The low-temperature rise of C is due to the contribution of the Eu^{151} and Eu^{153} nuclei [22]

$$C_N = b_N T^{-2} = Rx \sum_i a_i \frac{I_i + 1}{3 I_i} \left[\frac{\mu_i B_{\text{eff}}}{k_B T}\right]^2 \quad (1)$$

with the gas constant R and a_i, I_i, and μ_i, respectively, representing the relative abundance, nuclear spin, and the nuclear magnetic moment of the i-th Eu isotope. B_{eff} for the samples with $x = 0.3$ and $x = 0.65$ was obtained by linear interpolation between the values for Eu^{++} in SrTe and EuTe [23]. The resulting coefficient b_N will be used throughout in the following analysis of the magnetic specific heat.

Above $T \approx 400$ mK, the specific heat of EuTe rises much faster than $\propto T^3$ as expected for magnons in an isotropic antiferromagnet. In a reduced temperature

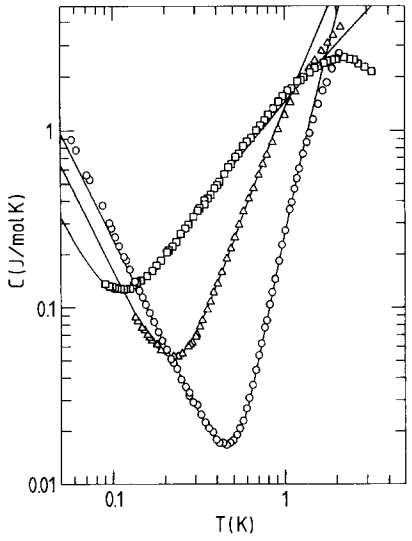

Fig. 2. Specific heat C vs. temperature T of the $Eu_xSr_{1-x}Te$ samples with $x=0.3$ (□), 0.65 (△), and 1 (○), and fits of (5), (6), and (4), respectively, to the data (see main text)

range

$$C=b_N T^{-2}+a_5 T^5 \tag{2}$$

fits the data satisfactorily, but this T dependence of C is not typical for antiferromagnets. A better interpretation of the behavior of C can be obtained assuming a weak anisotropy. This leads to an energy gap ΔE in the magnon density of states which results in an exponential decrease of the magnetic specific heat with decreasing temperature for $T \ll \Delta E/k_B$:

$$C=b_N T^{-2}+a_0 \exp(-\Delta E/k_B T) \tag{3}$$

However, a better description of the data is obtained incorporating a T^3 term, as found previously for the strongly anisotropic antiferromagnet $EuAs_3$ [20].

$$C=b_N T^{-2}+a_3 T^3 \exp(-\Delta E/k_B T) \tag{4}$$

The specific heat obtained from (4) with the parameters $a_3=1.14\,\mathrm{J/molK^4}$ and $\Delta E/k_B=1.49\,\mathrm{K}$ is plotted in Fig. 2, which is the best description of C for $T<1\,\mathrm{K}$. This suggests that the temperature dependence of the specific heat of EuTe is indeed due to magnetic anisotropy. The worse fits obtained with (2) and (3) are not shown.

The spin-glass sample $Eu_{0.3}Sr_{0.7}Te$ with a freezing temperature $T_f \approx 1\,\mathrm{K}$ [13] also shows anisotropic behavior in the specific heat with

$$C=b_N T^{-2}+aT\exp(-\Delta E/k_B T) \tag{5}$$

with $a=1.62\,\mathrm{J/molK^2}$ and $\Delta E/k_B=0.12\,\mathrm{K}$. This temperature dependence of C has first been seen for spin-glass samples of $Eu_xSr_{1-x}As_3$ [21]. The small energy gap for $x=0.3$ indicates a strong decrease of the anisotropy with dilution as previously observed for $Eu_xSr_{1-x}As_3$.

For the sample with $x=0.65$ one might expect an intermediate behavior:

$$C=b_N T^{-2}+aT^q \exp(-\Delta E/k_B T) \tag{6}$$

with $1<q<3$ and $0.12\,\mathrm{K}<\Delta E<1.49\,\mathrm{K}$. However, because of the additional parameter q, a fit is less reliable. For $q=2$ one obtains $\Delta E/k_B=0.33\,\mathrm{K}$ and $a=1.8\,\mathrm{J/molK^3}$. This curve is also shown in Fig. 2.

In summary, the specific heat at low temperatures gives evidence for anisotropy in pure EuTe and even in the spin-glass sample. The magnitude and the dependence of the energy gap ΔE on dilution are comparable to the behavior found in $Eu_xSr_{1-x}As_3$.

III.B. Specific heat in the vicinity of the transition temperature

Figure 3 shows the specific heat of $Eu_xSr_{1-x}Te$ for each concentration investigated in the temperature range $1.4\,\mathrm{K}<T<15\,\mathrm{K}$. For samples with $x \geqq 0.5$ a sharp peak occurs at the transition from the paramagnetic to the antiferromagnetic phase. For $x=1$ it has a clear λ-like shape. With dilution ($x<1$) the transition temperature and the height of the anomaly decrease and the peak develops towards a sharp cusp with a roughly linear $|t|$-dependence for $x=0.55$ (inset of Fig. 3), here $t=(T-T_c)/T_c$, $T_c=T_N$. The curves of the samples with $x=0.45$ and $x=0.3$ exhibit only rounded maxima. In general, the transition temperatures determined by the magnetic measurements in [12] coincide well with the temperatures of the anomaly in the specific heat (cf. Fig. 1). The deviations are small and probably due to thermometry. Only for the sample with $x=0.45$ the difference between the two temperatures is significant. This probably arises from the fact that this sample belongs to the spin-glass regime of the dilution series because in spin-glasses the maximum in the specific heat is usually observed at temperatures above the freezing temperature T_f.

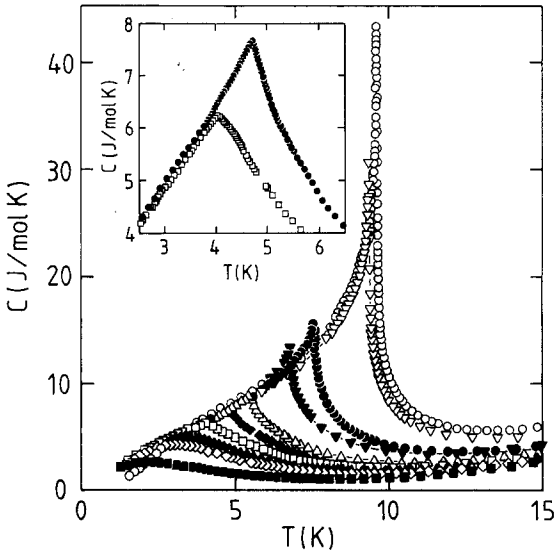

Fig. 3. Specific heat C vs. temperature T of all investigated $Eu_xSr_{1-x}Te$ samples for $1.4\,\mathrm{K}<T<15\,\mathrm{K}$. Because of the high density of data points, not all data are shown. x: ○ 1.00; ▽ 0.95; ● 0.80; ▼ 0.75; △ 0.65; ◆ 0.60; □ 0.55; ▲ 0.50; ◇ 0.45; ■ 0.30. Inset: Specific heat of the samples with $x=0.55$ (□) and 0.60 (●) in the vicinity of the antiferromagnetic transition

Table 1. Experimental parameters for $Eu_xSr_{1-x}Te$. The units of T_c and δT_c are K, of A', B and E are $Jmol^{-1}K^{-1}$, the unit of ξ_0 is Å. The three data sets for $x=1$ indicate three different fitting ranges. Symbols are explained in main text near (7) and (8)

$Eu_xSr_{1-x}Te$	T_c	$\lvert t\rvert_{min}$, $\lvert t\rvert_{max}$	δT_c	ξ_0	$\alpha=\alpha'$	A/A'	A'	B	$E=E'$
$x=1$	9.801 ±0.003	0.0015, 0.01	-	-	0.38 ±0.1	1.22 ±7.3	0.601 ±0.45	4.36[a] ±6	15 ±2
$x=1$	9.801 ±0.003	0.01, 0.06	-	-	0.0085 ±0.003	0.971 ±0.13	3.800 ±0.1	−436 ±200	15 ±2
$x=1$	9.8035 ±0.003	0.004, 0.1	-	-	0.055 ±0.005	0.838 ±0.1	3.573 ±0.1	−54.7 ±20	8 ±8
$x=0.95$	9.363 ±0.004	0.006, 0.08	0.01	285	0.025 ±0.03	0.922 ±0.25	3.034 ±0.1	−112 ±150	6.273 ±5
$x=0.80$	7.545 ±0.02	0.007, 0.2	0.03	205	−0.255 ±0.02	1.977 ±0.3	2.907 ±0.25	18.69 ±6	6.774 ±2
$x=0.75$	6.822 ±0.02	0.01, 0.2	0.017	276	−0.325 ±0.02	2.495 ±0.3	2.302 ±0.25	14.40 ±0.3	6.640 ±2
$x=0.65$	5.485 ±0.03	0.02, 0.15	0.055	154	−0.56 ±0.03	5.171 ±0.25	1.432 ±0.2	9.259 ±0.1	6.529 ±2
$x=0.60$	4.749 ±0.03	0.05, 0.3	0.07	133	−0.66 ±0.05	2.877 ±0.5	2.240 ±0.25	7.965 ±0.1	3.38 ±2
$x=0.55$	4.04 ±0.05	0.02, 0.3	0.035	214	−0.93 ±0.1	1.745 ±0.3	3.644 ±0.3	6.340 ±0.03	1.38 ±1
$x=0.5$	3.33 ±0.15	0.05, 0.5	-	-	−1.26 ±0.3	1.242 ±0.3	4.898 ±0.3	5.146 ±0.005	1.21 ±1

[a] For this fit $B' \neq B$ had to be assumed, with $B' = 19.85 \pm 5$

The rise of C at higher temperatures is due to the lattice contribution to C. From measurements up to 30 K (not shown) a Debye temperature $\theta_D = 180$ K for $x=1$ is obtained in good agreement with θ_D calculated from sound velocity measurements [24]. θ_D increases systematically with decreasing x to $\theta_D = 195$ K for $x=0.3$, due to the decreasing average atomic mass.

The specific-heat data for $x \geqq 0.5$ in the vicinity of T_N are evaluated with the function [3]

$$C(t) = (A/\alpha)\,|t|^{-\alpha} + B + Et \tag{7}$$

for $T > T_c$. The same function with the parameters A', α', B', and E' is employed to describe the data for $T < T_c$. RG calculations yield $\alpha = \alpha'$, $B = B'$, and $E = E'$ [3]. The remaining parameters α, A, A', B and E are obtained by fitting (7) to both sets of data $t > 0$ and $t < 0$ to yield common best-fitting parameters α, B (with some reservations for EuTe, see below) and E, while A and A' are allowed to differ from each other.

The sign of the curvature of a plot of $(C - Et)$ vs. $\log|t|$ gives directly the sign of α ($\alpha > 0$: positive curvature; $\alpha = 0$ straight line, logarithmic singularity; $\alpha < 0$: negative curvature). The constraint $\alpha = \alpha'$ implies same curvature for $T > T_c$ and $T < T_c$. As an example for negative α, C of $Eu_{0.75}Sr_{0.25}Te$ is shown in Fig. 4. Changes of the curvature occur for large $|t|$ on account of the regular contribution Et. The upper limit of $|t|$ is determined by the validity of the approximations which have been made to obtain (7) (neglect of singular terms of higher order, linear approximation of regular terms Et). The terms $(A/\alpha)\,|t|^{-\alpha}$ and B in (7) have a different meaning for $\alpha < 0$ and $\alpha > 0$. For $\alpha < 0$, B is the maximum value of C at $|t| = 0$ and becomes large for small negative α, while $(A/\alpha)\,|t|^{-\alpha}$ is finite and negative. For $\alpha > 0$, $(A/\alpha)\,|t|^{-\alpha}$ diverges at $|t| = 0$. For large $\alpha > 0$, B converges to the value of the regular contributions to C at $|t| = 0$, only $(A/\alpha)\,|t|^{-\alpha}$ describes the anomaly. Because of the singularity of (7) at $\alpha = 0$, the change of meaning of the parameters may lead to large negative fitting parameters of B for small $\alpha > 0$. This is observed for $x=1$ in the outer $|t|$-ranges and for $x=0.95$ (see Table 1).

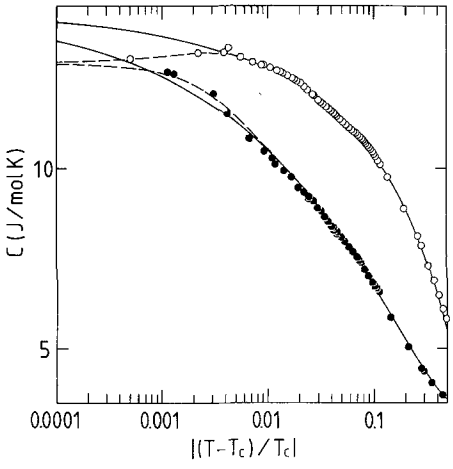

Fig. 4. Specific heat C vs. the reduced temperature $|t|$ of $Eu_{0.75}Sr_{0.25}Te$. The solid lines are fits to (7) with the parameters given in Table 1. Dashed lines include the T_c-smearing of (8). ○ $T < T_c$; ● $T > T_c$

As can be seen in Fig. 4, the curvature changes also for small $|t|$ presumably because of sample inhomo-

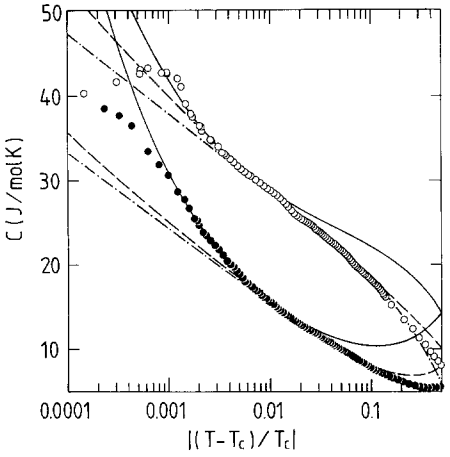

Fig. 5. Specific heat C vs. the reduced temperature $|t|$ of EuTe. The lines are fits to (7) with the parameters given in Table 1. Dashed-dotted line: $\alpha = 0.0085$, solid line: $\alpha = 0.38$, dashed line: fit with effective exponent $\alpha = 0.055$. o $T < T_c$; • $T > T_c$

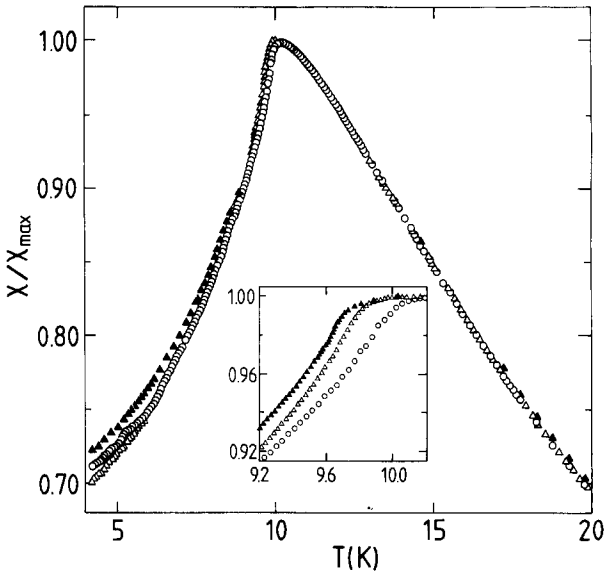

Fig. 6. Magnetic susceptibility χ vs. temperature T of EuTe for different orientation of the magnetic field relative to the sample. o $B\,||\,[001]$; △ $B\,||\,[\bar{1}11]$; ▲ $B\,||\,[111]$. Inset: χ in the vicinity of the Néel temperature

geneities. It is well-known that for $A/A' \neq 1$, concentration fluctuations lead to a rounding of the cusp of C and furthermore shift the apparent temperature of the maximum to a temperature smaller than T_c. Because of these effects, care has to be taken in choosing the t range used for the evaluation of α. To check the correct choice of the lower $|t|$ limit, the specific heat is calculated with function (7) under the additional assumption of a Gaussian distribution of subsystems with critical temperature T_c, volume $V(T_c)$, and variance δT_c:

$$V(T_c) = V_0 \exp[-(T_c - T_{c0})^2/2(\delta T_c)^2] \tag{8}$$

with the critical temperature T_{c0} of the ideal system. The dashed curve in Fig. 4 is the result for the sample with $x = 0.75$ with $T_{c0} = (6.822 \pm 0.02)$ K and $\delta T_c = 0.017$ K ($\delta T_c/T_c = 2.5 \cdot 10^{-3}$). Equation (8) describes the data very close to T_{c0} very well, i.e., the additional parameter δT_c describes the rounding *without* changing the other fitting parameters.

According to theoretical results of Chang and Hohenemser [26], the rounding of the cusp is caused by the cutoff of the correlation length ξ at a maximum value ξ_0 because of concentration fluctuations. With δT_c and the concentration dependence of the transition temperature dT_c/dx, it is possible to calculate this cutoff length, e.g., $\xi_0 \approx 280$ Å for $Eu_{0.75}Sr_{0.25}Te$. The fitting parameters for all samples are shown in Table 1.

For the samples with $x = 1$ and $x = 0.95$, positive exponents are found. Figure 5 displays the C vs. $\log|t|$ plot for EuTe. One notes a clear increase of the slope of C approaching T_c for $0.001 < |t| < 0.01$. This cannot be explained by sample inhomogeneities which lead to the maximum at $|t| \approx 0.001$ for the data $t < 0$ as discussed above but is an intrinsic feature of EuTe. Measurements performed on several samples confirm this. This might indicate a cross-over to a different fixed point very close to T_c. While $\alpha = 0.0085 \pm 0.003$ for $0.01 < |t| < 0.08$, for smaller reduced temperatures $0.0015 < |t| < 0.01$ one obtains $\alpha = 0.38 \pm 0.1$ (cf. Fig. 5). This cross-over was not observed in previous work. Although some deviations from Heisenberg behavior were found [7]. For the fit at smaller $|t|$, the constraint $B = B'$ could not be fulfilled, therefore the apparent value of α only describes the increase of the critical exponent and is not a meaningful fit to the data. The large positive critical exponent of the specific heat is in contradiction to the expectation for isotropic magnets, which in the light of the results of Sect. III.A, might not be too surprising. Also, the magnetic-field dependence of C shows anisotropic behavior (Sect. III.A). Additional indications for anisotropy are found in the magnetic susceptibility χ measured in external field $B = 0.1$ mT after zero-field cooling. The measurements have been performed on a spherical sample in order to avoid an influence of the sample geometry as, e.g., inhomogeneous internal fields. χ at $4\,\text{K} < T < 8\,\text{K}$ splits for different orientations of the applied field. The smallest χ at low T is observed for $B\,||\,[\bar{1}11]$, the highest for $B\,||\,[111]$, with χ for $B\,||\,[001]$ in between. This means that the plane which contains the $[\bar{1}11]$ direction is the easy plane of the magnetic structure in this sample with particular domain configuration whereas the [111] and [001] directions lie out of the easy plane. The inset of Fig. 6 shows the anisotropy of the Néel temperature. For $B\,||\,[\bar{1}11]$ and [001] a slightly higher T_N is observed as for $B\,||\,[111]$. Compared to the $(B-T)$ phase diagram (Fig. 11) this decrease in very low fields seems somewhat large. The reason for this is not understood.

A possible explanation for the deviations of α from Heisenberg behavior is thus the anisotropy because of magnetic dipole-dipole-interaction, which prevents the transversal spin fluctuations from growing to infinity. The complicated anisotropy in EuTe might be the reason that neither Ising ($\alpha = +0.11$) nor XY-behavior ($\alpha = -0.008$) [14] is observed, but a transition with a large critical exponent ≈ 0.3–0.4 very close to T_c. A more detailed account of the critical behavior of pure EuTe will be given elsewhere [27].

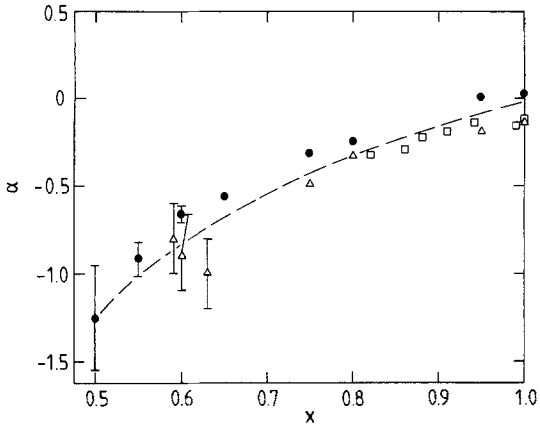

Fig. 7. Critical exponent α of the specific heat vs. the Eu-concentration of $Eu_xSr_{1-x}Te$ ● and $Eu_xSr_{1-x}S$ (△□ triangles from [4] and squares from [28]). The dashed line is intended as a guide to the eye only

In order to compare the result of α of EuTe to the exponents of the samples with $x < 1$ where no cross-over is observed, the data of EuTe of the temperature range $0.004 < |t| < 0.1$ were used to calculate an effective exponent $\alpha = 0.055$. This is the same $|t|$ range as used for the concentrated samples ($x \geqq 0.8$). The result is also plotted in Fig. 5. The optical agreement of this fit with the data is satisfactory, but its R.M.S. error is twice as large as for the fits for the other samples.

The concentration dependence α vs. x is shown in Fig. 7 together with the critical exponents for $Eu_xSr_{1-x}S$ [4, 28]. Because of the similar critical concentration in both systems ($Eu_xSr_{1-x}S$: $x_c = 0.51$, $Eu_xSr_{1-x}Te$: $0.45 \leqq x_c \leqq 0.5$), a normalization of the concentration axis is not necessary.

As Fig. 7 shows, α decreases continuously with concentration down to $\alpha \approx -1$ for the critical concentration $x \approx 0.5$. Because of the slightly rounded maximum for the sample with $x = 0.5$, the estimation of T_N has a considerable error and the value for α is only a crude approximation. Compared to the data of $Eu_xSr_{1-x}S$, α for $Eu_xSr_{1-x}Te$ exhibits a similar concentration dependence but systematical higher values. This enhancement of the critical exponent may again be caused by anisotropy in the telluride system. For both $Eu_xSr_{1-x}S$ and $Eu_xSr_{1-x}Te$ the result is in apparent contradiction to the Harris criterion. For $\alpha_0 > 0$ the Harris criterion predicts quite generally a change of the critical behavior with disorder while for $\alpha_0 < 0$ no change should occur. Hence for the latter, α shold not decrease further with dilution once having become zero near $x \approx 0.9$. For both systems, the experimental data agree with calculations by Heuer and Wagner [17] and Sobotta and Wagner [18] which yield a variation of an effective exponent α with concentration leading to $\alpha = -1$ at the critical concentration. Independent of the sign of α_0, it is important to note that the effective exponent is calculated for t in the experimentally attainable range $10^{-4} < |t| < 10^{-1}$. The similarity between the sulfide and the telluride systems seems to be a manifestation of intrinsic properties of these dilution series, regardless of whether the pure system exhibits $\alpha_0 > 0$ or $\alpha_0 < 0$. Of course, the asymptotic exponents differ for both cases. A possible origin of this "universality" could be the presence of competing interactions $J_1 > 0$ and $J_2 < 0$. To test this supposition, investigations are underway on the dilution system $Eu_xSr_{1-x}O$ where only ferromagnetic interactions exist [1]. Investigations of structurally disordered ferromagnets [29] always show unchanged "pure" critical exponents β and γ (in t ranges closer to T_c than specific-heat measurements allow) in agreement with the Harris criterion.

III.C. Specific heat in magnetic fields

To illustrate the low-temperature specific heat in magnetic fields, two typical samples $x = 0.65$ and $x = 0.3$ are discussed. Figure 8 shows the specific heat of $Eu_{0.65}Sr_{0.35}Te$ in several magnetic fields parallel to the [100] axis for $0.1\,K < T < 30\,K$. The anomaly at T_N is shifted to lower temperatures by applying a magnetic field. This field dependence is used to determine a magnetic phase diagram of $Eu_xSr_{1-x}Te$ (see below). First we will describe the low-temperature specific heat in magnetic fields. In $B = 3$ T the specific heat is suppressed compared to the zero field results, while in the larger field $B = 6$ T, $C(T)$ is enhanced even above the zero-field values. Figure 9 displays the specific heat of the spin-glass sample with $x = 0.30$ in various magnetic fields. In a magnetic field the zero-field anomaly located at $T \approx 2\,T_f$ is shifted to higher temperatures. Both effects are typical properties of nonmetallic spin-glasses as, e.g., $Eu_xSr_{1-x}S$ with $x \leqq 0.51$ [30]. An interesting feature of the specific heat of the sample with $x = 0.30$ (Fig. 9) is the crossing of the $C(T)$ curves in $B = 1.4$ T and 2.8 T. Both curves are lower than the specific heat without external field. Finally, in $B = 5.3$ T, C is smaller than in all other fields.

As described in Sect. I, EuTe in small fields is a canted antiferromagnet with varying angles between the spins and the applied field, depending on the magnitude of the field. The anisotropy apparently still exists in the diluted samples. A given applied field generates a different spin

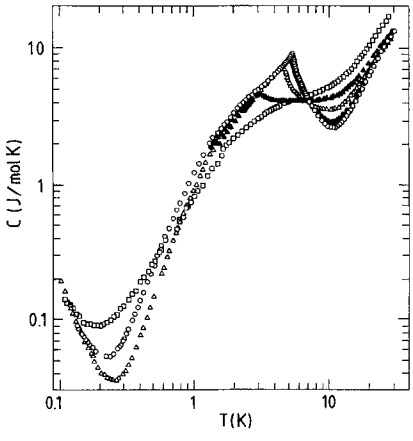

Fig. 8. Specific heat C vs. temperature T of $Eu_{0.65}Sr_{0.35}Te$ in magnetic fields. ○ $B = 0$ T; ● $B = 1.5$ T; △ $B = 3.0$ T; ▲ $B = 4.5$ T; □ $B = 6.0$ T

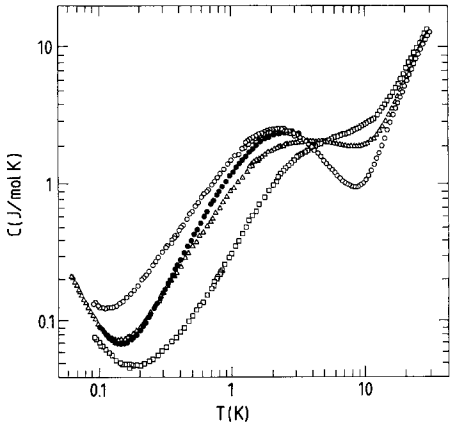

Fig. 9. Specific heat C vs. temperature T of $Eu_{0.30}Sr_{0.70}Te$ in magnetic fields. ○ $B=0$ T; ● $B=1.4$ T; △ $B=2.8$ T; □ $B=5.3$ T

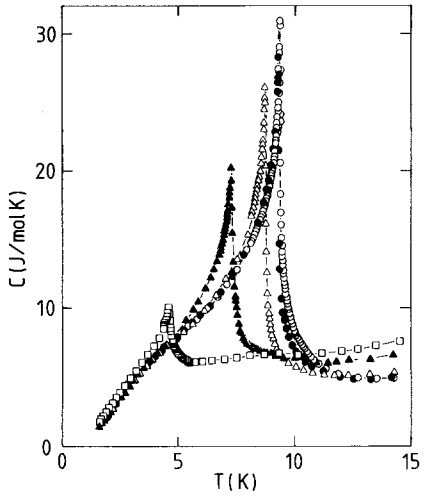

Fig. 10. Specific heat C vs. temperature T of $Eu_{0.95}Sr_{0.05}Te$ for $1.4\,K < T < 15\,K$ in magnetic fields. Dashed curves are guides to the eye only. □ $B=6.0$ T; ▲ $B=4.5$ T; △ $B=3.0$ T; ● $B=1.5$ T; ○ $B=0$ T

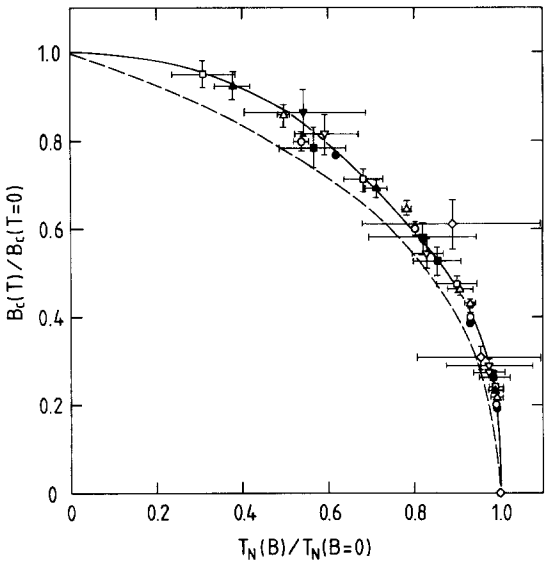

Fig. 11. Normalized phase boundary $B_c(T)/B_c(T=0)$ vs. $T_N(B)/T_N(B=0)$ of $Eu_xSr_{1-x}Te$ with $x \geqq 0.5$. The solid line is a guide to the eye relating to the data, the dashed curve represents the mean-field calculation from [1] normalized to $B_c(T=0)$ and $T_N(B=0)$ determined experimentally. x: ○ $x=1.00$, $B\,||\,(100)$; ● $x=1.00$, $B\,||\,(010)$; △ $x=0.95$; ▲ $x=0.80$; □ $x=0.75$; ■ $x=0.65$; ▽ $x=0.60$; ▼ $x=0.55$; ◇ $x=0.50$

configuration with an excitation spectrum depending on dilution. On the basis of the concentration dependence of the critical field (see below), the specific heat of $x=0.65$ in $B=3$ T and of $x=0.3$ in $B=1.4$ T should be compared with each other, whereas C for $x=0.65$ in $B=6$ T corresponds to the specific heat of $x=0.3$ in $B=2.8$ T. The smaller field enhances the anisotropy, the larger one reduces it again.

The reduction of C for $x=0.3$ in $B=5.3$ T is presumably due to the opening of an energy gap induced by the applied field, as observed, e.g., for spin-glasses of the $Eu_xSr_{1-x}S$-series [18].

Figure 10 shows the specific heat of $Eu_{0.95}Sr_{0.05}Te$ at temperatures $1.4\,K < T < 15\,K$ in different magnetic fields parallel to the [100] axis up to 6 T. The transition temperature is shifted to lower temperatures, the maximum of the anomaly at T_N is somewhat suppressed, but the anomaly itself remains narrow. The slight rounding might be due to the nonellipsoidal shape of the sample, the internal field is not homogeneous.

With the $T_N(B)$-data of the antiferromagnetic samples a normalized phase boundary $B_c(T)/B_c(T=0)$ vs. $T_N(B)/T_N(B=0)$ can be obtained (Fig. 11). The critical fields $B_c(T=0)$ are extrapolated from the $T_N(B)$ measurements for each concentration. The errors of this extrapolation yield the vertical error bars in Fig. 1. The horizontal error bars describe the uncertainty in the determination of $T_N(B)$, which is larger for the more diluted samples. The data points of all samples with $x \geqq 0.5$ lie on the same universal curve, i.e., the gross behavior of the transition remains the same in spite of increasing disorder and decreasing anisotropy.

The dashed curve in Fig. 11 represents results of mean-field calculations for the $T_N(B)$ phase boundary for EuTe, but assuming $S=\infty$ [11]. They yield a smaller critical field and a lower transition temperature than the experiments show. Therefore the calculated mean-field phase-boundary is normalized to the data at $T_N(B=0)$ and for $B_c(T=0)$. The significant deviations of the calculation, in particular at low temperatures and large fields, which also occur in Monte-Carlo simulations are due to the assumption of classical spins in both calculations [11].

IV. Conclusions

EuTe shows anisotropic behavior in various properties: the critical exponent shows a cross-over with a large positive value close to T_c; the specific heat at very low temperatures indicates an energy gap in the magnetic excitation spectrum; and the magnetic susceptibility in small fields depends on the direction of the field. The critical exponent of the specific heat α of EuTe does not agree with theoretical predictions probably because of the weak

anisotropy. The anisotropy can be traced down in the low-temperature specific heat of the diluted sample with $x = 0.65$ and is even visible for a spin-glass sample with $x = 0.30$.

The concentration dependence α vs. x of $Eu_xSr_{1-x}Te$ corresponds to that found earlier in $Eu_xSr_{1-x}S$ with α approaching -1 for $x \approx 0.5$ and underlines the influence of disorder on the apparent critical behavior of diluted magnets, but it deviates from results for structurally disordered magnets.

The dependence of the transition temperature on the external magnetic field yields a universal normalized magnetic phase boundary for all samples with $x \geqq 0.50$.

We would like to thank K. Fischer for providing the samples, T. Auerswald for performing the susceptibility measurements, and K. Binder and H. Claus for helpful discussions.

References

1. Zinn, W.: J. Magn. Magn. Mater. **3**, 23 (1976)
2. Maletta, H.: J. Appl. Phys. **53**, 2185 (1982); Maletta, H., Zinn, W.: In: Handbook of the physics and chemistry of rare earths, Vol. 12. Gschneidner, K.A. Jr., Eyring, L. (eds.) Amsterdam: North Holland 1986
3. Kornblit, A., Ahlers, G., Buehler, E.: Phys. Rev. **B17**, 282 (1978); Kornblit, A., Ahlers, G.: Phys. Rev. **B11**, 2678 (1975)
4. Wosnitza, J., Löhneysen, H. v.: Europhys. Lett. **10**, 381 (1989)
5. In contrast to [3] where $\alpha = -0.04$ was found for EuO, new experimental results reveal a critical behavior that is explicable with pure 3d Heisenberg exponents and an additional rounding near T_c due to inhomogeneities (cf. Sect. III.B). Wosnitza, J., Stroka, B., Scheer, E., Löhneysen, H. v.: (to be published)
6. Kötzler, J., Scheithe, W.: J. Magn. Magn. Mater. **54–57**, 649 (1986)
7. Johanson, W.R., McCollum, D.C.: Phys. Rev. **B22**, 2435 (1980); Westerholt, K., Sobotta, G.: J. Phys. **F13**, 2371 (1983); Westerholt, K.: J. Magn. Magn. Mater. **54–57**, 721 (1986)
8. Oliveira, N.F. Jr., Foner, S., Shapira, Y., Reed, T.B.: Phys. Rev. **B5**, 2634 (1970)
9. Will, G., Robert, S.J., Alperin, H.A., Nathans, R.: J. Phys. Chem Solids **24**, 1679 (1963)
10. Battles, J.W., Everett, G.E.: Phys. Rev. **B1**, 3021 (1970)
11. Nowotny, R.M., Binder, K.: Z. Phys. B - Condensed Matter **77**, 287 (1989)
12. Börgermann, F.J., Maletta, H.: Phys. Rev. **B35**, 8454 (1987); see also: Börgermann, F.J.: Thesis, Köln 1986; Reports of KFA Jülich Nr. 2042
13. Zinn, H.G., Weizen, H., Syassa, K.: Phys. Rev. **B32**, 4066 (1985)
14. Le Guillou, J.C., Zinn-Justin, J.: Phys. Rev. Lett. **39**, 95 (1977); Le Guillou, J.C., Zinn,-Justin, J.: Phys. Rev. **B21**, 3976 (1980)
15. Kornblit, A., Ahlers, G.: Phys. Rev. **B8**, 5163 (1973)
16. Harris, A.B.: J. Phys. **C7**, 1671 (1974); Stinchcombe, R.B.: In: Phase transitions and critical phenomena, Vol. 7, pp. 151. Domb, C., Lebowitz, J.L. (eds.). New York: Academic Press 1983
17. Heuer, H.O., Wagner, D.: Phys. Rev. **B40**, 2502 (1989)
18. Sobotta, G., Wagner, D.: J. Phys. **C11**, 1467 (1978); Sobotta, G., Wagner, D.: J. Magn. Magn. Mater. **28**, 1 (1982)
19. Löhneysen, H. v., Berg, R. van den, Lecomte, G.V., Zinn, W.: Phys. Rev. **B31**, 2920 (1985)
20. Fischer, J., Schröder, A., Löhneysen, H. v., Bauhofer, W., Steigenberger, U.: Phys. Rev. **B39**, 11775 (1989)
21. Schröder, A., Löhneysen, H. v., Bauhofer, W.: Phys. Rev. Lett. **57**, 622 (1986)
22. Freeman, A.J., Watson, R.E.: In: Magnetism, Vol. IIa. Rado, G.T., Suhl, H. (eds.). New York: Academic Press 1965
23. Sauer, Ch., Zinn, W.: Physica **86–88**, 1031 (1977); Crecelius, G., Maletta, H., Pink, H., Zinn, W.: J. Magn. Magn. Mater. **5**, 150 (1977)
24. Shapira, Y., Reed, B.: AIP Conf. Proc. **5**, pt. 2, 837 (1972)
25. Kreps, L.W., Friedberg, S.A.: J. Low Temp. Phys. **26**, 317 (1977); Jaccarino, V., King, A.R.: J. Phys. (Paris) **49**, C8-1209 (1988)
26. Scheer, E., Wosnitza, J., Löhneysen, H. v., Kürsch, R., Lang, M., Steglich, F.: (to be published)
27. Chang, X.S., Hohenemser, C.: Phys. Rev. **B37**, 261 (1988)
28. Haeiwa, T., Kita, E., Siratori, K., Kohn, K., Tasaki, A.: J. Phys. Soc. Jpn. **57**, 3381 (1988)
29. Kellner, W.U., Fähnle, M., Kronmüller, H., Kaul, S.N.: Phys. Status Solidi (b) **144**, 397 (1987); Fähnle, M., Braun, P., Reisser, R., Seeger, M., Kronmüller, H.: J. Phys. (Paris) **49**, C8-1201 (1988)
30. Wosnitza, J., Löhneysen, H. v., Zinn, W., Krey, U.: Phys. Rev. **B33**, 3436 (1986)